

# The dynamical structure factor of a fermionic supersolid on an optical lattice

Ettore Vitali,<sup>1,2</sup> Patrick Kelly,<sup>1</sup> Annette Lopez,<sup>1</sup> Gianluca Bertaina,<sup>3,4</sup> and Davide Emilio Galli<sup>3</sup>

<sup>1</sup>*Department of Physics, California State University Fresno, Fresno, California 93740*

<sup>2</sup>*Department of Physics, The College of William and Mary, Williamsburg, Virginia 23187*

<sup>3</sup>*Dipartimento di Fisica, Università degli Studi di Milano, via Celoria 16, 20133 Milano, Italy*

<sup>4</sup>*Istituto Nazionale di Ricerca Metrologica, Strada delle Cacce 91, 10135 Torino, Italy*

We perform a Quantum Monte Carlo study of a spin-balanced two-dimensional cold Fermi gas on an optical lattice, which can be experimentally realized with laser standing waves. The system is modeled with a Hubbard hamiltonian with on-site attractive interaction. At half-filling, when on average one fermion occupies each lattice site, the system displays an intriguing supersolid phase: a superfluid with a checkerboard density modulation. Interfacing unbiased Auxiliary-Field Monte Carlo simulations with state-of-art analytic continuation techniques, we compute the density dynamical structure factor  $S(\mathbf{q}, \omega)$  of the system, in order to characterize the dynamical properties of this supersolid phase. We find evidence of the existence of two collective modes, which we interpret as arising from the two broken symmetries in the system:  $s$ -wave pairing superfluidity coexists with a non-uniform local density. The mapping  $U \rightarrow -U$  in the Hubbard model makes these results important for the repulsive model as well. Furthermore, this work paves the way for an investigation of the behavior of the model when we move away from half-filling, either changing the density or introducing a spin polarization.

## I. INTRODUCTION

Cold atomic gases provide an unprecedented opportunity to explore many-body physics and unravel phenomena that arise from the interplay among quantum mechanics, quantum statistics and interatomic forces [1, 2]. These gases are unique in the amazing degree of experimental control which is possible over the physical parameters. Different microscopic hamiltonians can be engineered, and the interatomic forces can be tuned through the Feshbach resonance mechanism. The systems can be embedded in several kinds of external fields, including optical lattices [3, 4] and synthetic magnetic fields [5]. This unprecedented control allows us to mimic experimental conditions that can be found in some of the most mysterious systems in the universe, like unconventional superconductors or nuclear matter inside neutron stars, just to mention two examples [6–8], by tuning a few easily adjustable parameters to achieve the desired force law and thermodynamic state. Furthermore, we have the unique possibility to explore new phases of matter, like exotic superfluid phases that, in some cases, may even display important topological properties [9].

One very intriguing phase that can be investigated with cold atoms is the supersolid, where superfluidity coexists with crystalline order. This phase has been an object of speculation for a few decades and was predicted in several theoretical studies going back to the '70s [10, 11]. Historically, the first candidate in the quest for supersolidity in realistic systems was  $^4\text{He}$  and a huge interest was triggered in the early 2000s [12], when several experimental groups were able to detect non-classical rotational inertia in solid  $^4\text{He}$ . Unfortunately, follow up experiments supported by the vast majority of theoretical works proved that the ground state of bulk solid  $^4\text{He}$  is not a superfluid. We now have strong evidence that  $^4\text{He}$  can be found in either a superfluid or a crystalline

phase, but the two phases do not coexist [13]. The next candidate is naturally a Bose-Einstein condensate realized with cold atoms. Although, at first sight, the diluteness of such a system appears to rule out the possibility of having a stable crystalline phase, a supersolid phase was observed in Bose-Einstein condensates coupled with light [14–16]; moreover, very recently exciting theoretical and experimental results were published clearly indicating the possibility of realizing a supersolid by engineering a combination of a short-range repulsion and a long-range dipolar interatomic potential [17–22].

Interestingly, it has been known for quite a long time that a supersolid phase can also be found in fermionic systems. In fact, if we confine a fermionic cold gas, made of Lithium or Potassium atoms, in a quasi two-dimensional geometry where an optical lattice is generated using laser standing waves, it is expected that a supersolid state of matter can be realized if the particle density is accurately tuned in such a way that, on average, we have one fermion in each valley of the optical lattice. This condition is referred to as "half-filling". In the '90s a seminal paper on the two-dimensional attractive Hubbard model, which is known to be an accurate model of the experimental situation described above, predicted the stability of such a phase [23]. Quantum Monte Carlo (QMC) calculations for the attractive Hubbard model at half-filling provided evidence for long range order both in the density-density correlations, implying the system is a solid, and in the pairing correlation, implying a superfluid phase [4, 23]. Incidentally, we mention that numerical simulations predict that the supersolid state realized with cold atoms on an optical lattice is stable only at half-filling, while the crystalline order immediately melts as the particle density is changed [4, 23].

As it is well known from the study of  $^4\text{He}$  and its celebrated phono-rotonic dispersion relation of density fluctuations, a crucial property of any superfluid

is the spectrum of density fluctuations, which is contained in the dynamical structure factor  $S(\mathbf{q}, \omega)$  of the system. The calculation of  $S(\mathbf{q}, \omega)$  for a supersolid two-dimensional cold Fermi gas on an optical lattice at zero temperature is the main focus of this paper. We perform the study using cutting edge Auxiliary-Field Quantum Monte Carlo (QMC) techniques [24] interfaced with state of the art analytic continuation techniques [25, 26]. With QMC we perform an *exact* calculation of the intermediate scattering function in imaginary time; in this context, *exact* means that we are able to tune the parameters of the methodology in such a way that the systematic error is below the level of statistical uncertainty. We stress that this is quite unique for fermionic systems and is made possible by the particular formulation of the Auxiliary-Field QMC which is free of the celebrated sign problem for the attractive Hubbard model, as long as we study spin balanced systems [27]. In particular, we exploit recent methodological advancements in the Auxiliary-Field QMC technique that allow us to compute exact dynamical correlations in imaginary time with a very favorable scaling as a function of the size of the system [27–29]. The analytic continuation, which is necessary to estimate properties in real time, in particular  $S(\mathbf{q}, \omega)$ , is performed using the Genetic Inversion via Falsification of Theories (GIFT) technique [25, 26], which has been proved to provide robust results for quantum many-body systems [28, 30–33].

Through a comparison with the results for the non-interacting Hubbard model at half-filling, we find evidence that the interaction gives rise to a very interesting well defined collective mode  $\omega(\mathbf{q})$  emerging from the particle-hole background and resembling a phononic spectrum, clearly suggesting that the particles move coherently in the supersolid phase. The mode has a "rotonic" minimum at  $\mathbf{q} = (\frac{\pi}{a}, \frac{\pi}{a})$ ,  $a$  being the lattice parameter, whose frequency vanishes in the thermodynamic limit, corresponding to a crystalline checkerboard order. At higher energy, our results are consistent with the existence of an intriguing second collective mode: we interpret the presence of the two modes as a consequence of the two symmetries that are broken in the supersolid phase [19–22, 34, 35], and namely the translational symmetry and the  $U(1)$  symmetry. The fate of these modes when we move away from half-filling, either changing the density or introducing some spin polarization, will be the subject of future studies.

It is important to observe that, although our main focus is the attractive Hubbard model and its supersolid phase, our results are also very important for the repulsive model: in fact, if we change the sign of the interaction in the Hamiltonian, a well known mapping transforms the supersolid phase into an antiferromagnetic phase, as the particle density is mapped into the spin density. We will discuss this in more detail below. In regard to this, we hope that our results will provide useful benchmarks for other methodologies, both in the realm of many-body theories and in computer simula-

tions.

The paper is structured as follows: in Section II we will introduce the microscopic model of the system and we will briefly describe the Quantum Monte Carlo method, together with the analytic continuation technique. In Section III we will present our results for  $S(\mathbf{q}, \omega)$ , together with other important correlation functions for the physical system. In Section IV we will discuss the broad significance of our results and the importance for condensed matter physics. Finally, we will draw our conclusions in Section V.

## II. MODEL AND METHOD

We model the system using the two-dimensional Hubbard hamiltonian, describing a collection of structureless fermions with spin 1/2 moving on a lattice, representing the optical lattice which is experimentally realized with standing waves of laser light:

$$\begin{aligned}\hat{H} &= \hat{K} + \hat{V} \\ \hat{K} &= -t \sum_{\langle \mathbf{r}, \mathbf{r}' \rangle, \sigma} \hat{c}_{\mathbf{r}, \sigma}^\dagger \hat{c}_{\mathbf{r}', \sigma} \\ \hat{V} &= U \sum_{\mathbf{r}} \hat{n}_\uparrow(\mathbf{r}) \hat{n}_\downarrow(\mathbf{r})\end{aligned}\quad (1)$$

with:

$$\hat{n}_\sigma(\mathbf{r}) = \hat{c}_{\mathbf{r}, \sigma}^\dagger \hat{c}_{\mathbf{r}, \sigma}. \quad (2)$$

In Eq. (1),  $\mathbf{r}$  runs over the sites of a square lattice made of  $\mathcal{N}_s = L \times L$  sites, defined by the minima of the optical lattice, while  $\sigma$  is the spin orientation. The first term in the hamiltonian Eq. (1) is the kinetic energy, describing particles hopping among nearest-neighbor lattice sites with amplitude  $t$ , while the second term is the on-site interaction, whose strength is given by the parameter  $U$ . In this paper, we will focus on the attractive case, and thus  $U < 0$ . The symbol  $\langle \mathbf{r}, \mathbf{r}' \rangle$  means that the sites are nearest neighbors. We will use periodic boundary conditions throughout this paper. The Hubbard model [36, 37] is one of the most widely studied models in atomic physics and in condensed matter physics. Despite its apparent simplicity, no analytical solutions to this hamiltonian are known in more than one dimension. Although in most applications the Hubbard model has a repulsive interaction, related to Coulomb force, also the attractive case is extremely interesting, both in the realm of cold atoms and in condensed matter physics [38].

The main purpose of this paper is to compute the dynamical structure factor of the system at zero temperature:

$$S(\mathbf{q}, \omega) = \frac{1}{N} \int_{-\infty}^{+\infty} \frac{dt}{2\pi} \left\langle \Psi_0 \left| e^{it\hat{H}} \hat{n}_{\mathbf{q}} e^{-it\hat{H}} \hat{n}_{-\mathbf{q}} \right| \Psi_0 \right\rangle \quad (3)$$

where  $|\Psi_0\rangle$  is the ground state of (1), while  $\hat{n}_{\mathbf{q}}$  is the

Fourier component of the density of particles:

$$\hat{n}_{\mathbf{q}} = \sum_{\mathbf{k}, \sigma} \hat{c}_{\mathbf{k}, \sigma}^\dagger \hat{c}_{\mathbf{k}+\mathbf{q}, \sigma}. \quad (4)$$

All the momenta,  $\mathbf{q}$  and  $\mathbf{k}$  belong to the first Brillouin zone of the square lattice,  $[-\frac{\pi}{a}, \frac{\pi}{a}] \times [-\frac{\pi}{a}, \frac{\pi}{a}]$ . All the lengths in this paper will be measured in units of  $a$  and, therefore, we will set  $a = 1$  from now on. Since our numerical approach requires us to work with finite lattices of linear size  $L$  and we choose periodic boundary conditions, the momenta are discretized:  $\mathbf{k} = \frac{2\pi}{L} \mathbf{n}$ , where  $\mathbf{n} \in \mathbb{Z}^2$ .

Computing Eq. (3) for a correlated quantum system is a huge challenge: in this work, we will use the cutting-edge Auxiliary-Field QMC technique to sample at the same time both the ground state wave function of the system  $|\Psi_0\rangle$  and the propagator in imaginary time  $\exp(-\tau\hat{H})$ : this will allow us to compute exactly the intermediate scattering function in imaginary time, as discussed below. We will then use the Genetic Inversion via Falsification of Theories (GIFT) to perform the analytic continuation necessary to compute  $S(\mathbf{q}, \omega)$ .

The Auxiliary-Field QMC technique relies on the projection formula:

$$|\Psi_0\rangle \propto \lim_{\beta \rightarrow +\infty} e^{-\beta(\hat{H}-E_0)}|\phi_0\rangle \quad (5)$$

which allows us to asymptotically project a given approximation  $|\phi_0\rangle$  to the ground state wave function of the system onto the ground state itself. In (5)  $E_0$  is an estimate of the ground state energy while the approximation  $|\phi_0\rangle$  is chosen to be a Slater determinant with  $N_\uparrow$  spin-up and  $N_\downarrow$  spin-down particles, such that  $|\phi_0\rangle$  is not orthogonal to the  $\mathcal{N}_p$ -particle ( $\mathcal{N}_p = N_\uparrow + N_\downarrow$ ) ground state  $|\Psi_0\rangle$  of (1). In the simplest case,  $|\phi_0\rangle$  is simply the ground state wave function of the non-interacting Hubbard model. In this work we will focus on the behavior of the model at half-filling, which means that  $\mathcal{N}_p = L \times L$ , and without spin polarization, meaning  $N_\downarrow = N_\uparrow$ .

Starting from a Trotter decomposition:

$$e^{-\beta(\hat{H}-E_0)} = \left(e^{-\delta\tau(\hat{H}-E_0)}\right)^M, \quad \delta\tau = \frac{\beta}{M} \quad (6)$$

which allows us to rely on the behavior of the propagator for small imaginary time  $\delta\tau$ , the Auxiliary-Field QMC method uses an Hubbard-Stratonovich transformation which yields the following expression:

$$e^{-\delta\tau(\hat{H}-E_0)} \simeq \int d\mathbf{x} p(\mathbf{x}) \hat{B}(\mathbf{x}) \quad \delta\tau \rightarrow 0 \quad . \quad (7)$$

In Eq. (7) the integrations runs over all the possible configurations of an auxiliary field  $\mathbf{x}$  defined on the lattice: in our case,  $\mathbf{x}$  is an Ising field,  $x(\mathbf{r}) = \pm 1$ . The function  $p(\mathbf{x})$  is a uniform probability density on the space of the configurations of the auxiliary field:  $p(\mathbf{x}) = \frac{1}{2^{\mathcal{N}_p}}$ . An explicit expression for the operator  $\hat{B}(\mathbf{x})$  appearing in (7)

is given by the following [39]:

$$\hat{B}(\mathbf{x}) = e^{\delta\tau E_0} e^{-\delta\tau \hat{K}/2} \prod_{\mathbf{r}} \hat{b}_{\mathbf{r}}(x(\mathbf{r})) e^{-\delta\tau \hat{K}/2} \quad (8)$$

where  $\hat{K}$  is the kinetic energy of the Hubbard model, while:

$$\hat{b}_{\mathbf{r}}(x) = e^{-\delta\tau U(\hat{n}(\mathbf{r})-1)/2} e^{\gamma x(\hat{n}(\mathbf{r})-1)} \quad (9)$$

with  $\hat{n}(\mathbf{r}) = \hat{n}_\uparrow(\mathbf{r}) + \hat{n}_\downarrow(\mathbf{r})$  being the particle density operator while  $\cosh(\gamma) = \exp\left(\frac{\delta\tau|U|}{2}\right)$ . From the point of view of the physical interpretation, the Hubbard-Stratonovich transformation allows us to map the interacting problem onto an ensemble of non-interacting systems of fermions moving in random external potentials. The average over the ensemble recovers the fully interacting model. From the point of view of implementation, the key point of the methodology is the fact that the operator  $\hat{B}(\mathbf{x})$  defined in Eq. (8) is the exponential of a one-body operator dependent on the auxiliary field configuration. This implies that the operator  $\hat{B}(\mathbf{x})$  maps Slater determinants into Slater determinants. This allows the QMC procedure to implement a random walk whose state space coincides with the manifold of Slater determinants with  $\mathcal{N}_p$  particles. Such a random walk opens the possibility to compute expectation values of any physical property, say  $\hat{O}$ , using Monte Carlo integration, relying on the expression:

$$\langle \hat{O} \rangle \simeq \frac{\int d\mathbf{x}_1 \dots d\mathbf{x}_{2M} \pi(\mathbf{x}_0, \dots, \mathbf{x}_{2M}) \mathcal{O}(\mathbf{x}_0, \dots, \mathbf{x}_{2M})}{\int d\mathbf{x}_1 \dots d\mathbf{x}_{2M} \pi(\mathbf{x}_0, \dots, \mathbf{x}_{2M})} \quad (10)$$

where  $\langle \hat{O} \rangle$  is shorthand for  $\langle \Psi_0 | \hat{O} | \Psi_0 \rangle$ , while:

$$\begin{aligned} \pi(\mathbf{x}_1, \dots, \mathbf{x}_{2M}) &= \prod_{i=1}^{2M} p(\mathbf{x}_i) \langle \phi_L | \phi_R \rangle \\ \mathcal{O}(\mathbf{x}_1, \dots, \mathbf{x}_{2M}) &= \frac{\langle \phi_L | \hat{O} | \phi_R \rangle}{\langle \phi_L | \phi_R \rangle}. \end{aligned} \quad (11)$$

The “left” and “right” Slater determinants are defined as:

$$\begin{aligned} \langle \phi_L | &= \langle \phi_0 | \hat{B}(\mathbf{x}_{2M}) \dots \hat{B}(\mathbf{x}_{M+1}) \\ | \phi_R \rangle &= \hat{B}(\mathbf{x}_M) \dots \hat{B}(\mathbf{x}_1) | \phi_0 \rangle. \end{aligned} \quad (12)$$

In the simplest implementation of the methodology, we use the non-interacting wave function as the initial wave function:

$$|\phi_0\rangle = \prod_{\mathbf{k}, \sigma} \hat{c}_{\mathbf{k}, \sigma}^\dagger |0\rangle \quad (13)$$

where  $\varepsilon(\mathbf{k}) = -2t(\cos(k_x) + \cos(k_y))$  is the dispersion relation of the non-interacting two-dimensional Hubbard model,  $\varepsilon_F$  is the Fermi energy, while the operator:

$$\hat{c}_{\mathbf{k}, \sigma}^\dagger = \frac{1}{\sqrt{\mathcal{N}_s}} \sum_{\mathbf{r}} e^{i\mathbf{k} \cdot \mathbf{r}} \hat{c}_{\mathbf{r}, \sigma}^\dagger \quad (14)$$

creates one particle with spin orientation  $\sigma$  in a plane wave  $e^{i\mathbf{k}\cdot\mathbf{r}}/\sqrt{N_s}$ . In the state  $|\phi_0\rangle$ , all the orbitals of the particles in the system will be plane-waves. The Slater determinant  $|\phi_R\rangle$ , for a given imaginary time dependent configuration of the auxiliary-field  $(\mathbf{x}_1, \dots, \mathbf{x}_{2M})$  will be obtained from  $|\phi_0\rangle$ , by applying the product of the operators  $\hat{B}(\mathbf{x}_i)$  to the plane waves, once for each particle in the system. Similarly we build  $\langle\phi_L|$ . Each Slater determinant  $|\phi\rangle$  is parametrized as  $\Phi = \Phi^\uparrow \otimes \Phi^\downarrow$  where  $\Phi^\sigma$  is a  $N_s \times N_\sigma$  complex matrix, containing all the components  $\langle\mathbf{r}, \sigma|\phi\rangle$ . The matrix elements  $\mathcal{O}$  are obtained with simple linear algebra manipulations. This is the essence of the QMC method: we randomly sample imaginary time dependent configurations of the auxiliary-field and this allows us to implement a random walk in the manifold of the Slater determinants for  $N_p$  particles; an average over all the possible random walks yields physical properties of the correlated systems. Several technical improvements can make the technique more efficient, including importance sampling and force bias [27, 40]. The resulting methodology has a very favorable scaling as a function of the size of the system: precisely it scales as  $\mathcal{O}(N_p^2 N_s)$ . It is important to mention that, for the spin-balanced ( $N_\uparrow = N_\downarrow$ ) attractive Hubbard model, the method is sign-problem free, which implies that we can compute exact physical properties of the system. By exact we mean that, for a given choice of  $N_p$  and  $N_s$ , we can always choose the parameters of the Quantum Monte Carlo run, and namely the time step  $\delta\tau$  and the total projection time  $\beta = M\delta\tau$ , in such a way that the systematic error is smaller than the statistical uncertainty for a given computation time. The Auxiliary-Field QMC method can be extended to the calculation of dynamical properties. As described in detail in the papers [28, 29], it is possible to compute exactly dynamical correlations in imaginary time, like the intermediate scattering function:

$$F(\mathbf{q}, \tau) = \langle \Psi_0 | e^{\tau\hat{H}} \hat{n}_{\mathbf{q}} e^{-\tau\hat{H}} \hat{n}_{-\mathbf{q}} | \Psi_0 \rangle \quad (15)$$

without effecting the favorable scaling of the methodology. This is easily achieved since the imaginary time evolution operator  $e^{-\tau\hat{H}}$  is the same operator that allows us to sample the ground state wave function using the projection formula (5), and the same formal manipulations can be applied to it. This results in an efficient algorithm to compute  $F(\mathbf{q}, \tau)$ , with the same complexity that is required by static calculations. We use the intermediate scattering function from Quantum Monte Carlo as an input for the analytic continuation problem, that is needed to estimate the dynamical structure factor  $S(\mathbf{q}, \omega)$  through the relation:

$$F(\mathbf{q}, \tau) = \int_0^{+\infty} d\omega e^{-\tau\omega} S(\mathbf{q}, \omega). \quad (16)$$

We stress one more time that our calculations of  $F(\mathbf{q}, \tau)$  are unbiased, as no sign problem exists for the spin-balanced attractive Hubbard model in the framework

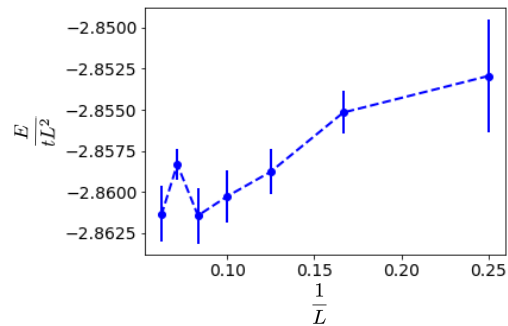


FIG. 1. (Color online) Energy per site of the Hubbard model at half-filling for  $U/t = -4$  as a function of  $1/L$ , where  $L$  is the linear size of the system. The energies are in units of the hopping amplitude  $t$ .

of the Auxiliary-Field QMC methodology. We use the state-of-art Genetic Inversion via Falsification of Theories (GIFT) [25, 26] method to estimate the dynamical structure factor  $S(\mathbf{q}, \omega)$  starting from  $F(\mathbf{q}, \tau)$ . We improve the accuracy of the procedure by including the  $f$ -sum rule, which will be discussed in appendix A. This method has been widely employed to study dynamical properties of superfluid  $^4\text{He}$  in different dimensionalities [25, 26, 30, 32], normal  $^3\text{He}$  [33], cold atomic systems [28, 31, 34, 41] and the Hubbard model [29], and it is known to provide robust results. In the following section we will present our results.

### III. RESULTS

We study the attractive Hubbard model on a square lattice with  $N_s = L \times L$  sites hosting  $N_p$  particles at half-filling, that is  $N_p = N_s$  and spin balance. The strength of the interaction is chosen to be  $U/t = -4$ . Since we target bulk properties, it is crucial to perform size extrapolation, in order to make sure that the size effects are below the level of the statistical uncertainties in the Monte Carlo calculations. In Fig. 1 we plot the energy per site as a function of the linear size, for  $L = 4, 6, 8, 10, 12, 14, 16$ . The results clearly show that, within an uncertainty of the order of  $10^{-3}$  the energy per site converges to its bulk limit around  $L = 10$ . All the calculations that we will present will be for  $L = 12$ . All the other parameters of the simulations, like time-step and total projection time are tuned in such a way that the systematic error is below the level of the uncertainties in the Monte Carlo data.

Before presenting our results for the dynamical properties, which are the central product of this work, we present our results about the density correlation and the pairing correlations, defined respectively as:

$$C_n(\mathbf{r}) = \langle \Psi_0 | \hat{n}(\mathbf{r}) \hat{n}(0) | \Psi_0 \rangle \quad (17)$$

where  $\hat{n}(\mathbf{r}) = \hat{c}_{\mathbf{r},\uparrow}^\dagger \hat{c}_{\mathbf{r},\uparrow} + \hat{c}_{\mathbf{r},\downarrow}^\dagger \hat{c}_{\mathbf{r},\downarrow}$  and:

$$C_{pair}(\mathbf{r}) = \langle \Psi_0 | \hat{\Delta}^\dagger(\mathbf{r}) \hat{\Delta}(0) | \Psi_0 \rangle \quad (18)$$

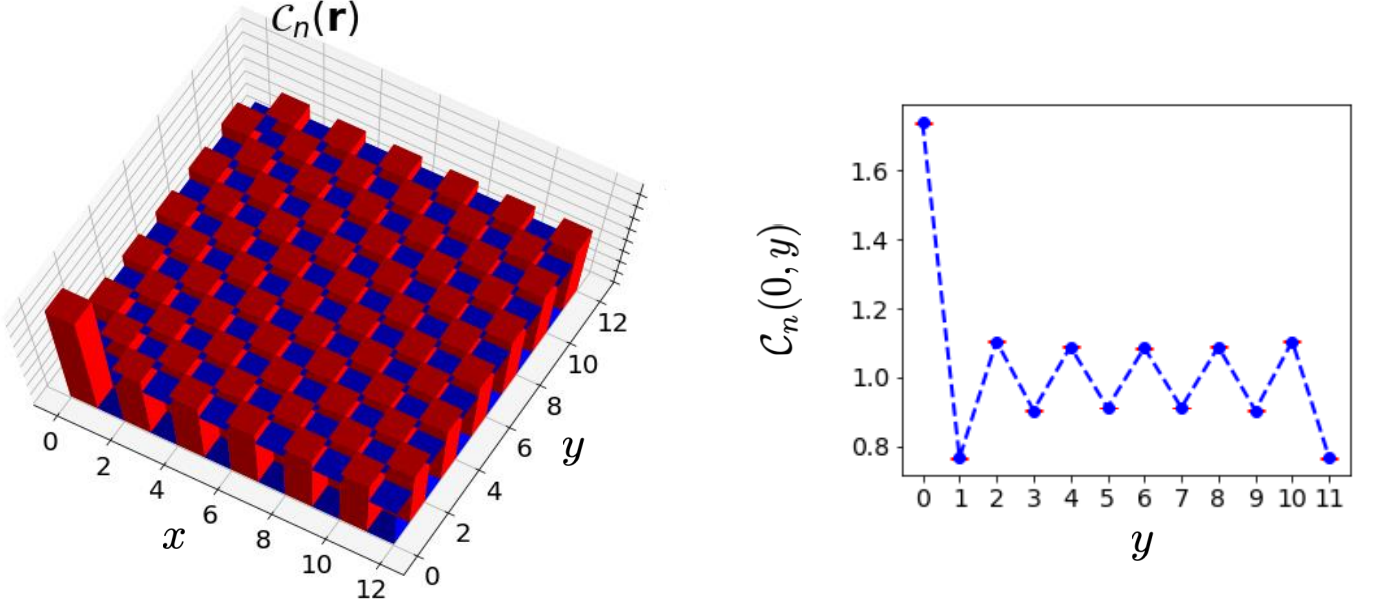


FIG. 2. (Color online) Left panel: density correlation  $C_n(\mathbf{r})$  (dimensionless) for the attractive Hubbard model with  $U/t = -4$  as a function of the position  $\mathbf{r} = (x, y)$ . Two colors have been chosen to aid the reader: red for higher density lattice sites and blue for lower density lattice sites. Right panel: a slice of the density correlation taken with  $x = 0$ . The uncertainties are plotted but may be difficult to see, as they are consistently below the size of the symbols.

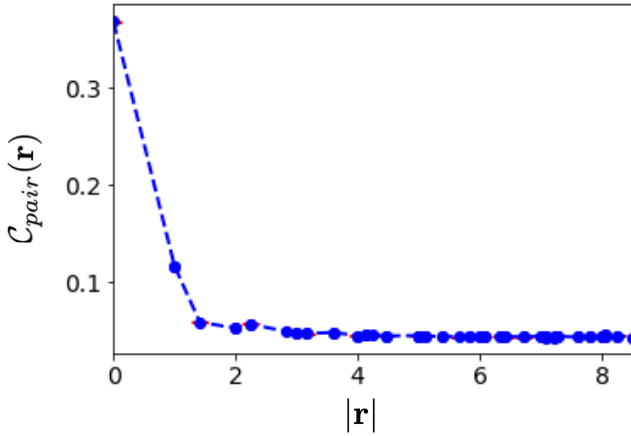


FIG. 3. (Color online) Pairing Correlation  $C_{pair}(\mathbf{r})$  for the attractive Hubbard model at half-filling with  $U/t = -4$  as a function of the distance  $|\mathbf{r}|$ . The uncertainties are plotted but may be difficult to see, as they are consistently below the size of the symbols.

where the on-site pairing is defined as:

$$\hat{\Delta}(\mathbf{r}) = \hat{c}_{\mathbf{r},\downarrow} \hat{c}_{\mathbf{r},\uparrow}. \quad (19)$$

The density correlations, shown in Fig.2, exhibit clear long-range order. The system is in a crystalline phase, with a checkerboard modulation of the particle of wave vector  $\mathbf{q} = (\pi, \pi)$ ; that is, the order parameter has the

form:

$$n(\mathbf{r}) = 1 + A \cos(\mathbf{q} \cdot \mathbf{r}), \quad A < 1. \quad (20)$$

We observe that this is not the trivial order imposed by the optical lattice: it is a density modulation that arises from the interplay between interatomic correlations and nesting of the non-interacting Fermi surface at half-filling, as we will discuss in more detail below.

The pairing correlation is shown in Fig.3 as a function of distance  $|\mathbf{r}|$  and clearly displays convergence to a non-zero limit:

$$C_{pair}(\mathbf{r}) \rightarrow n_0^2, \quad |\mathbf{r}| \rightarrow +\infty. \quad (21)$$

This indicates the emergence of off-diagonal long range order, corresponding to a superfluid phase. The order parameter  $n_0$  plays the role of a condensate fraction. Intuitively, the singlet-pairs that form in the system as a consequence of the attractive interaction become coherent and form a Bose-Einstein condensate. We observe that the pairs have total spin equal to zero, and thus obey Bose statistics in the limit of strong attraction. The combination of the long-range orders in both the density and pairing correlations is the signature of a supersolid phase, which appears to be the equilibrium state at half-filling.

The central result of our paper is the calculation of the dynamical structure factor  $S(\mathbf{q}, \omega)$  of the system in this unique phase. In order to shed light into the physical information contained in  $S(\mathbf{q}, \omega)$ , we find it useful to show the results together with the non-interacting exact dynamical structure factor, which we denote  $S_0(\mathbf{q}, \omega)$  and

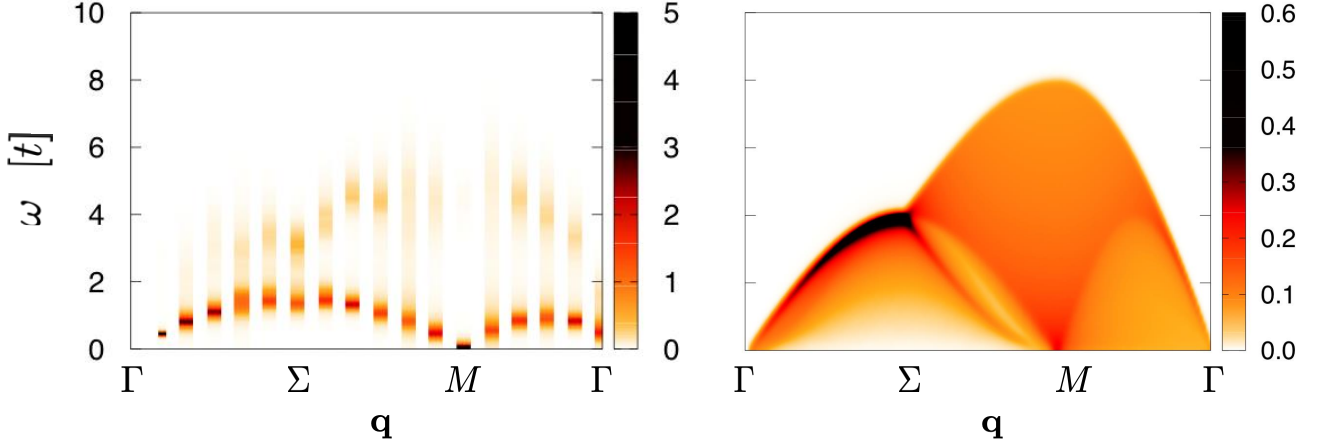


FIG. 4. (Color online) Left panel: color plot of the dynamical structure factor  $S(\mathbf{q}, \omega)$  (arbitrary units) for the attractive Hubbard model at half-filling with  $U/t = -4$  as a function of momentum  $\mathbf{q}$  along a triangle in the first Brillouin zone and frequency  $\omega$ , in units of the hopping amplitude  $t$ . Right panel: color plot of  $S_0(\mathbf{q}, \omega)$  (arbitrary units) for the non-interacting system at the same density. The points in the first Brillouin zone are labeled as  $\Gamma = (0, 0)$ ,  $\Sigma = (0, \pi)$ , and  $M = (\pi, \pi)$ .

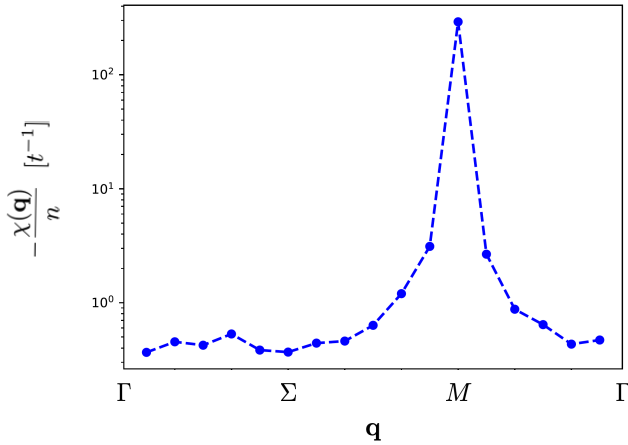


FIG. 5. (Color online) Density response function  $\chi(\mathbf{q})$ , as a function of the magnitude of the momentum vector  $\mathbf{q}$  of the density modulation imposed on the system, defined along a triangle in the first Brillouin zone. The points in the first Brillouin zone are labeled as  $\Gamma = (0, 0)$ ,  $\Sigma = (0, \pi)$ , and  $M = (\pi, \pi)$ . The uncertainties, on this scale, are below the size of the symbols.

which is given by:

$$S_0(\mathbf{q}, \omega) = \frac{1}{2\pi^2} \int_{[-\pi, \pi]^2} d\mathbf{k} \delta(\omega - (\varepsilon(\mathbf{k} + \mathbf{q}) - \varepsilon(\mathbf{k}))) \{ \theta(\varepsilon_F - \varepsilon(\mathbf{k})) (1 - \theta(\varepsilon_F - \varepsilon(\mathbf{k} + \mathbf{q}))) \} \quad (22)$$

where  $\varepsilon(\mathbf{k}) = -2t(\cos k_x + \cos k_y)$  is the dispersion relation of the Hubbard model, while  $\varepsilon_F$  is Fermi energy, which vanishes at half-filling due to particle-hole symmetry. The results are shown in Fig. 4, where the interacting  $S(\mathbf{q}, \omega)$  is shown in the left panel, while the non-interacting  $S_0(\mathbf{q}, \omega)$  is plotted in the right panel. The mo-

mentum runs along the triangle in the first Brillouin zone defined by the vertices  $\Gamma = (0, 0)$ ,  $\Sigma = (0, \pi)$ ,  $M = (\pi, \pi)$ . The non-interacting dynamical structure factor captures all the particle-hole excitations allowed by the dispersion relation  $\varepsilon(\mathbf{k})$ ; we stress that, at half-filling, the Fermi surface is defined by the equation  $\varepsilon(\mathbf{k}) = 0$  and has a characteristic diamond shape. It displays an important nesting property, related to the wave vector  $(\pi, \pi)$ : if a momentum  $\mathbf{k}$  belongs to the Fermi surface at half-filling, then  $\mathbf{k} + (\pi, \pi)$  still belongs to the Fermi surface. This is the reason for the fact that  $S_0((\pi, \pi), \omega = 0)$  does not vanish: it is possible to transfer momentum  $(\pi, \pi)$  at zero energy cost. This generates an instability towards a state of modulated density, which becomes stable as soon as we switch the interaction on. The stability of the ordered phase in the interacting system appears very clearly as a peak of  $S((\pi, \pi), \omega)$  at  $\omega = 0$ . We stress that, as the lattice that we are simulating is finite, the peak at  $\mathbf{q} = (\pi, \pi)$  is at a finite but very small  $\omega$  and tends to zero in the thermodynamic limit. For the  $12 \times 12$  system, we estimate that the peak has an energy  $\omega(\pi, \pi) \lesssim 10^{-2} t$ .

Very interestingly, from the comparison between the non-interacting dynamical structure factor and the interacting  $S(\mathbf{q}, \omega)$  we immediately see that, in the interacting system, most of the spectral weight becomes concentrated around a well defined collective mode  $\omega(\mathbf{q})$ . This mode has a clear phononic shape and displays a “roton” minimum at  $\mathbf{q} = (\pi, \pi)$ , which vanishes in the thermodynamic limit and corresponds to the checkerboard crystalline structure of the system. Our data strongly suggest that  $\omega(\mathbf{q}) \rightarrow 0$  also as  $\mathbf{q} \rightarrow 0$ , although the smallest momentum that we considered is  $\mathbf{q} = (\frac{\pi}{6}, 0)$  due to the finite size of the lattice. We observe that the mode  $\omega(\mathbf{q})$  has a broadening, with a width on the order of  $0.5t$ , which arises from the possible decay of the mode into

particle-hole excitations and from uncertainty in the analytic continuation method. We also see an interesting higher energy branch, carrying smaller spectral weight; the existence of two modes can be expected in a supersolid [34, 35] if we consider that the system is breaking at the same time translational symmetry, giving rise to the crystalline order, and  $U(1)$  symmetry, giving rise to the pairing order. The intensity of the higher energy mode appears to be very small close to  $\mathbf{q} = (\pi, \pi)$ , which can be a consequence of its decay in the particle-hole continuum. We also notice, in the interacting system, an evident depletion of the particle-hole continuum below the coherent mode, which thus cannot decay into simple particle-hole excitations.

This mode  $\omega(\mathbf{q})$ , together with the higher energy mode, emerging from the broad particle-hole continuum typical of a non-interacting fermionic system as we switch on the interatomic interaction is a spectacular manifestation of quantum coherence. As soon as the particles start to attract each other, the fermions start to organize in pairs. These pairs form a Bose-Einstein condensate and the coherent fluid of pairs organize in a spatially modulated density pattern. The modes that we found describes the low energy dynamics of this very unique quantum system.

Finally, in Fig. 5 we show our result for the density response function:

$$\chi(\mathbf{q}) = -n \int_0^{+\infty} d\omega \frac{S(\mathbf{q}, \omega)}{\omega} \quad (23)$$

where  $n$  is the particle density, equal to one in our case. Physically,  $\chi(\mathbf{q})$  is the linear response function describing the response of the particle density to an external potential trying to impose to the system a density modulation with wave-vector  $\mathbf{q}$ . The function appears to be smooth as a function of  $\mathbf{q}$ , apart from the divergence at  $\mathbf{q} = (\pi, \pi)$ , which is the momentum of the checkerboard crystalline order. We comment that the value  $\chi(\pi, \pi)$  that we obtain is large but finite, as we are simulating a finite system;  $\chi(\pi, \pi)$  diverges in the thermodynamic limit.

#### IV. DISCUSSION: RELEVANCE FOR REPULSIVE MODELS

We would like to take the opportunity here to stress that our results are not only significant for the attractive Hubbard model, and thus to the supersolid phase that can be realized with cold atoms on an optical lattice, but they are also relevant for the repulsive Hubbard model. In fact, if we consider the partial particle-hole transformation defined as:

$$\begin{aligned} \hat{d}_{\mathbf{r},\uparrow}^\dagger &= \hat{c}_{\mathbf{r},\downarrow}^\dagger \\ \hat{d}_{\mathbf{r},\downarrow}^\dagger &= (-1)^{\mathbf{r}} \hat{c}_{\mathbf{r},\downarrow} \end{aligned} \quad (24)$$

where  $(-1)^{\mathbf{r}} = (-1)^{x+y}$  if  $\mathbf{r} = (x, y)$  and we focus on the model at half-filling, the hamiltonian preserves the

form (1) with  $U \rightarrow -U$ . This can be easily proved by taking into account the fact that the square lattice is a bipartite lattice, through the following simple algebraic manipulations:

$$\begin{aligned} \hat{K} &= -t \sum_{\langle \mathbf{r}, \mathbf{r}' \rangle, \sigma} \hat{c}_{\mathbf{r},\sigma}^\dagger \hat{c}_{\mathbf{r}',\sigma} = -t \sum_{\langle \mathbf{r}, \mathbf{r}' \rangle, \sigma} \hat{d}_{\mathbf{r},\sigma}^\dagger \hat{d}_{\mathbf{r}',\sigma} \\ \hat{V} &= U \sum_{\mathbf{r}} \hat{c}_{\mathbf{r},\uparrow}^\dagger \hat{c}_{\mathbf{r},\uparrow} \hat{c}_{\mathbf{r},\downarrow}^\dagger \hat{c}_{\mathbf{r},\downarrow} = U \sum_{\mathbf{r}} \hat{d}_{\mathbf{r},\uparrow}^\dagger \hat{d}_{\mathbf{r},\uparrow} \hat{d}_{\mathbf{r},\downarrow}^\dagger \hat{d}_{\mathbf{r},\downarrow} \quad (25) \\ &= \frac{UL^2}{2} - U \sum_{\mathbf{r}} \hat{d}_{\mathbf{r},\uparrow}^\dagger \hat{d}_{\mathbf{r},\uparrow} \hat{d}_{\mathbf{r},\downarrow}^\dagger \hat{d}_{\mathbf{r},\downarrow} \end{aligned}$$

where in the last step we used the fact that we are at half-filling and that we work in the sector of the Hilbert space with  $N_\uparrow = \frac{L^2}{2}$ .

We observe that the fluctuation of the particle density is mapped onto the spin density along the  $z$  direction, perpendicular to the plane, since:

$$\begin{aligned} \hat{n}(\mathbf{r}) - 1 &= \hat{c}_{\mathbf{r},\uparrow}^\dagger \hat{c}_{\mathbf{r},\uparrow} + \hat{c}_{\mathbf{r},\downarrow}^\dagger \hat{c}_{\mathbf{r},\downarrow} - 1 \\ &= \hat{d}_{\mathbf{r},\uparrow}^\dagger \hat{d}_{\mathbf{r},\uparrow} - \hat{d}_{\mathbf{r},\downarrow}^\dagger \hat{d}_{\mathbf{r},\downarrow} = 2\hat{S}_z(\mathbf{r}). \end{aligned} \quad (26)$$

Also, the on-site pairing is mapped onto the (staggered) spin density along  $x$ -direction, in-plane, since:

$$\begin{aligned} \frac{1}{2} (\hat{\Delta}(\mathbf{r}) + \hat{\Delta}^\dagger(\mathbf{r})) &= \frac{1}{2} (\hat{c}_{\mathbf{r},\downarrow} \hat{c}_{\mathbf{r},\uparrow} + \hat{c}_{\mathbf{r},\uparrow}^\dagger \hat{c}_{\mathbf{r},\downarrow}^\dagger) \\ &= \frac{1}{2} ((-1)^{\mathbf{r}} \hat{d}_{\mathbf{r},\downarrow}^\dagger \hat{d}_{\mathbf{r},\uparrow} + (-1)^{\mathbf{r}} \hat{d}_{\mathbf{r},\uparrow}^\dagger \hat{d}_{\mathbf{r},\downarrow}) = (-1)^{\mathbf{r}} \hat{S}_x(\mathbf{r}). \end{aligned} \quad (27)$$

The important message is that our calculations provide exact results for the repulsive Hubbard model at half-filling. The superfluid phase that we detect in the attractive model from the pairing correlation function is mapped onto an antiferromagnetic order in the  $x$ -direction, in-plane. The crystalline phase, which we detect from the density correlation functions is mapped onto an antiferromagnetic order in the  $z$ -direction, perpendicular to the plane. Finally, the dynamical structure factor is mapped to the spin structure factor in the  $z$ -direction, and the collective modes that we found give information about the spectrum of spin density modulations in the repulsive system. We expect that our results provide important benchmarks also for the repulsive model, where several methodologies, like for example, just to mention a few, dual-fermions approaches [42], several generalization of dynamical mean field theories and slave bosons [43] are systematically used due to the importance of the model for unconventional superconductors. In particular, as most of the above mentioned methods work at finite temperature, our results can provide very useful benchmarks for the zero-temperature limit which, in general, is very hard to study using finite temperature approaches.

Before drawing our conclusions we would like to stress an important point: in the repulsive model, we expect



that in the bulk limit, due to isotropy, there is a degeneracy in the ground state corresponding to the possibility of rotating the antiferromagnetic order parameter through any angle. More formally, the model has  $SU(2)$  symmetry. Practically, we can have antiferromagnetic order with order parameter pointing along arbitrary directions in space. If we now consider the mapping  $U \rightarrow -U$  and go to the attractive model, the above mentioned symmetry unveils an interesting symmetry between crystalline order, which would correspond to antiferromagnetic order along the  $z$  direction and superfluid order, which would correspond to antiferromagnetic order along the  $x$  direction. In the supersolid phase both orders are present at the same time, which corresponds to antiferromagnetic order in the  $xz$  plane. This is very important as it makes the landscape fertile for novel exotic phases which may appear when we move from half-filling, either changing the particle density or breaking the spin balance. We plan to investigate this in future studies, both from the static and the dynamical point of view. This may pave the way for deep insights into the physics of pairing, with important applications both in cold atoms and in condensed matter physics.

## V. CONCLUSIONS

We used an exact methodology to sample the ground state of the attractive Hubbard model at half-filling. We computed density and pairing correlations in the bulk limit and confirmed the existence of a supersolid phase, with long-range order both in the density correlations, corresponding to a crystalline checkerboard order with wave vector  $\mathbf{q} = (\pi, \pi)$  and in the on-site pairing correlations, corresponding to a superfluid phase. Our central result was the study of the spectrum of density correlations of the system: we were able to compute exactly the intermediate scattering function in imaginary time and we used the state-of-art GIFT method to perform the analytic continuation necessary to obtain an estimation of the dynamical structure factor  $S(\mathbf{q}, \omega)$ . In order to shed light into the dynamical properties of the supersolid phase, we found useful to show a comparison with the non-interacting dynamical structure factor at the same density. We found interesting collective modes which arises when the interactions are switched on: one lower energy mode  $\omega(\mathbf{q})$  which clearly vanishes at  $\mathbf{q} = (\pi, \pi)$  and a higher energy branch, carrying less spectral weight: we interpret the two modes as related to the two symmetry breaking mechanisms that take place at the same time, leading to crystalline order and superfluidity. Although finite size effects do not allow us to have access to the limit  $\mathbf{q} \rightarrow 0$ , we expect that  $\omega(\mathbf{q})$  will vanish in that limit and the data appear to be consistent with this. Apart from the intrinsic interest of the supersolid phase that can be realized in fermionic cold atoms, we hope that our results will serve as useful benchmarks for correlated approaches to quantum systems, as our

calculations in imaginary time are unbiased, which is a very rare finding in many-body problems. Moreover, we expect that the relevance for repulsive models, together with the relevance of the Hubbard model in material science, will stimulate further research aiming at characterizing dynamical properties of many-body systems. Finally, we plan to investigate, in future studies, the behavior of the model as we move away from half-filling. In particular, we would like to allow the particle density to change, in order to see if there may be a density modulated phase which becomes stable at some values of the filling, and to break the spin balance, which is expected to allow the system to develop highly nontrivial pairing mechanisms, related to exotic phases like the Fulde-Ferrel-Larkin-Ovchinnikov phase.

One of us, E.V., acknowledges useful discussions with Shiwei Zhang, Peter Rosenberg, Hao Shi and Yuan-Yao He. Computing was carried out at the Extreme Science and Engineering Discovery Environment (XSEDE), which is supported by National Science Foundation grant number ACI-1053575. D.E.G. acknowledges the CINECA awards IskraB PANDA and IskraC RENNA for the availability of high performance computing resources and support.

## Appendix A: The $f$ -sum Rule for the Hubbard Model

In this appendix we will present some details about the analytic calculation of the  $f$ -sum rule for the Hubbard Hamiltonian. The main purpose is to obtain a simple expression for the first moment:

$$\mathcal{M}_1(\mathbf{q}) = \int_0^{+\infty} d\omega \omega S(\mathbf{q}, \omega) \quad (\text{A1})$$

the following exact expression holds:

$$\mathcal{M}_1(\mathbf{q}) = \frac{1}{2N} \left\langle \sum_{\mathbf{k}, \sigma} (\varepsilon(\mathbf{k} + \mathbf{q}) + \varepsilon(\mathbf{k} - \mathbf{q})) \hat{c}_{\mathbf{k}, \sigma}^\dagger \hat{c}_{\mathbf{k}, \sigma} - 2\hat{T} \right\rangle \quad (\text{A2})$$

where:

$$\hat{T} = \sum_{\mathbf{k}, \sigma} \varepsilon(\mathbf{k}) \hat{c}_{\mathbf{k}, \sigma}^\dagger \hat{c}_{\mathbf{k}, \sigma} \quad (\text{A3})$$

is the kinetic energy operator of the Hubbard model, with the usual dispersion relation:

$$\varepsilon(\mathbf{k}) = -2t \sum_{i=1}^d \cos(k_i) \quad (\text{A4})$$

with  $d$  being the dimensionality.

We stress that the result (A2) critically depends on the form of the dispersion relation and it reduces to the traditional  $f$ -sum rule when the quadratic dispersion is used. We also comment that (A2) cannot be evaluated analytically as this would require the calculation of the spin



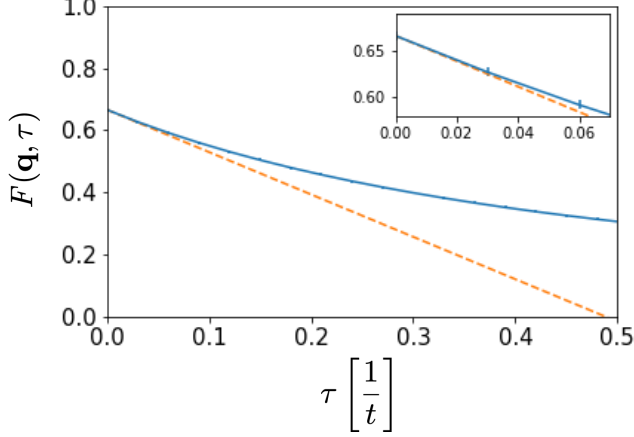


FIG. 6. (Color online) For  $\mathbf{q} = \frac{2\pi}{L}(3, 3)$  we show the comparison between the intermediate scattering function as computed from QMC (blue dots with errorbars connected by full line to guide the eye) and the straight line  $y(\tau) = F(\mathbf{q}, \tau = 0) - \tau \mathcal{M}_1(\mathbf{q})$ . We see that the line  $y(\tau)$  is clearly tangent to  $F(\mathbf{q}, \tau)$  at  $\tau = 0$ . The inset is just a zoom in.

resolved momentum distribution:  $n(\mathbf{k}, \sigma) = \langle \hat{c}_{\mathbf{k}, \sigma}^\dagger \hat{c}_{\mathbf{k}, \sigma} \rangle$ ; however this quantity can be easily obtained from a QMC simulation.

In order to derive (A2) we start from the expression:

$$S(\mathbf{q}, \omega) = \frac{1}{N} \sum_n \delta(\omega - (E_n - E_0)) |\langle \Psi_0 | \hat{n}_{\mathbf{q}} | \Psi_n \rangle|^2 \quad (\text{A5})$$

where  $\{|\Psi_n\rangle\}$  is an orthonormal basis of eigenvectors of

the Hamiltonian related to the eigenvalues  $\{E_n\}$ . Also:

$$\hat{n}_{\mathbf{q}} = \sum_{\mathbf{k}, \sigma} \hat{c}_{\mathbf{k}, \sigma}^\dagger \hat{c}_{\mathbf{k} + \mathbf{q}, \sigma} \quad (\text{A6})$$

is the Fourier transform of the local density of the particles.

From (A5) we immediately conclude that:

$$\mathcal{M}_1(\mathbf{q}) = \frac{1}{N} \sum_n (E_n - E_0) |\langle \Psi_0 | \hat{n}_{\mathbf{q}} | \Psi_n \rangle|^2. \quad (\text{A7})$$

This equality through simply algebraic manipulations can be recast as:

$$\mathcal{M}_1(\mathbf{q}) = \frac{1}{2N} \left\langle \left[ [\hat{n}_{\mathbf{q}}, \hat{H}], \hat{n}_{-\mathbf{q}} \right] \right\rangle. \quad (\text{A8})$$

The main result (A2) follows from the simple but lengthy explicit evaluation of the commutators.

The possibility to compute the first moment  $\mathcal{M}_1(\mathbf{q})$  is important for the analytic continuation procedure, as it allows us to improve the constraints in the GIFT method. The relation between the  $f$ -sum rule and the intermediate scattering function rests on the following equality:

$$\frac{\partial}{\partial \tau} F(\mathbf{q}, \tau = 0) = -\mathcal{M}_1(\mathbf{q}). \quad (\text{A9})$$

We find it useful to show in Fig. 6 that this relation is satisfied by our QMC calculations, this being a further cross-check for the accuracy of QMC. In fact, although there is no sign problem, making the results unbiased, the calculation of  $F(\mathbf{q}, \tau)$  requires the sampling of the imaginary time evolution, while  $\mathcal{M}_1(\mathbf{q})$  just requires static calculations, which are more straightforward. Relation (A9) provides a useful additional verification of the accuracy of the evaluation of  $F(\mathbf{q}, \tau)$ .

- 
- [1] S. Giorgini, L. P. Pitaevskii, and S. Stringari, *Rev. Mod. Phys.* **80**, 1215 (2008).
  - [2] I. Bloch, J. Dalibard, and W. Zwerger, *Rev. Mod. Phys.* **80**, 885 (2008).
  - [3] C. Gross and I. Bloch, *Science* **357**, 995 (2017).
  - [4] P. Rosenberg, H. Shi, and S. Zhang, *Phys. Rev. Lett.* **119**, 265301 (2017).
  - [5] Y.-J. Lin, R. L. Compton, K. Jimnez-Garca, J. V. Porto, and I. B. Spielman, *Nature* **462**, 628632 (2009).
  - [6] J. Carlson, S. Gandolfi, and A. Gezerlis, *Progress of Theoretical and Experimental Physics* **2012** (2012).
  - [7] P. van Wyk, H. Tajima, D. Inotani, A. Ohnishi, and Y. Ohashi, *Phys. Rev. A* **97**, 013601 (2018).
  - [8] P. T. Brown, D. Mitra, E. Guardado-Sanchez, R. Nourafkan, A. Reyembaut, C.-D. Hébert, S. Bergeron, A.-M. S. Tremblay, J. Kokalj, D. A. Huse, P. Schauß, and W. S. Bakr, *Science* **363**, 379 (2019).
  - [9] D.-W. Zhang, Y.-Q. Zhu, Y. X. Zhao, H. Yan, and S.-L. Zhu, *Advances in Physics* **67**, 253 (2018).
  - [10] A. J. Leggett, *Phys. Rev. Lett.* **25**, 1543 (1970).
  - [11] G. V. Chester, *Phys. Rev. A* **2**, 256 (1970).
  - [12] E. Kim and M. H. W. Chan, *Science* **305**, 1941 (2004).
  - [13] J. Choi, T. Tsui, D. Takahashi, H. Choi, K. Kono, K. Shirahama, and E. Kim, *Phys. Rev. B* **98**, 014509 (2018).
  - [14] J. Léonard, A. Morales, P. Zupancic, T. Donner, and T. Esslinger, *Science* **358**, 1415 (2017).
  - [15] J. Léonard, A. Morales, P. Zupancic, T. Esslinger, and T. Donner, *Nature* **543**, 87 (2017).
  - [16] J.-R. Li, J. Lee, W. Huang, S. Burchesky, B. Shteynas, F. Ç. Top, A. O. Jamison, and W. Ketterle, *Nature* **543**, 91 (2017).
  - [17] L. Tanzi, E. Lucioni, F. Famà, J. Catani, A. Fioretti, C. Gabbanini, R. N. Bisset, L. Santos, and G. Modugno, *Phys. Rev. Lett.* **122**, 130405 (2019).
  - [18] F. Böttcher, J.-N. Schmidt, M. Wenzel, J. Hertkorn, M. Guo, T. Langen, and T. Pfau, *Phys. Rev. X* **9**, 011051 (2019).
  - [19] L. Chomaz, D. Petter, P. Ilzhöfer, G. Natale, A. Trautmann, C. Politi, G. Durastante, R. M. W. van Bijnen,

- A. Patscheider, M. Sohmen, M. J. Mark, and F. Ferlino, Phys. Rev. X **9**, 021012 (2019).
- [20] G. Natale, R. M. W. van Bijnen, A. Patscheider, D. Pette, M. J. Mark, L. Chomaz, and F. Ferlino, Physical Review Letters **123**, 050402 (2019).
- [21] M. Guo, F. Böttcher, J. Hertkorn, J.-N. Schmidt, M. Wenzel, H. P. Büchler, T. Langen, and T. Pfau, Nature **574**, 386 (2019).
- [22] L. Tanzi, S. M. Roccuzzo, E. Lucioni, F. Famà, A. Fioretti, C. Gabbanini, G. Modugno, A. Recati, and S. Stringari, Nature **574**, 382 (2019).
- [23] R. T. Scalettar, E. Y. Loh, J. E. Gubernatis, A. Moreo, S. R. White, D. J. Scalapino, R. L. Sugar, and E. Dagotto, Phys. Rev. Lett. **62**, 1407 (1989).
- [24] S. Zhang, *Auxiliary-Field Quantum Monte Carlo for Correlated Electron Systems*, Vol. 3 of *Emergent Phenomena in Correlated Matter: Modeling and Simulation*, Ed. E. Pavarini, E. Koch, and U. Schollwöck (Verlag des Forschungszentrum Jülich, 2013).
- [25] G. Bertaina, D. E. Galli, and E. Vitali, Advances in Physics: X **2**, 302 (2017).
- [26] E. Vitali, M. Rossi, L. Reatto, and D. E. Galli, Phys. Rev. B **82**, 174510 (2010).
- [27] H. Shi, S. Chiesa, and S. Zhang, Phys. Rev. A **92**, 033603 (2015).
- [28] E. Vitali, H. Shi, M. Qin, and S. Zhang, Phys. Rev. A **96**, 061601 (2017).
- [29] E. Vitali, H. Shi, M. Qin, and S. Zhang, Phys. Rev. B **94**, 085140 (2016).
- [30] G. Bertaina, M. Motta, M. Rossi, E. Vitali, and D. E. Galli, Phys. Rev. Lett. **116**, 135302 (2016).
- [31] M. Motta, E. Vitali, M. Rossi, D. E. Galli, and G. Bertaina, Phys. Rev. A **94**, 043627 (2016).
- [32] F. Arrigoni, E. Vitali, D. E. Galli, and L. Reatto, Low Temp. Phys. **39**, 793 (2013).
- [33] M. Nava, D. E. Galli, S. Moroni, and E. Vitali, Phys. Rev. B **87**, 144506 (2013).
- [34] S. Saccani, S. Moroni, and M. Boninsegni, Phys. Rev. Lett. **108**, 175301 (2012).
- [35] S. Saccani, S. Moroni, E. Vitali, and M. Boninsegni, Mol. Phys. **109**, 2807 (2011).
- [36] J. Hubbard, Proceedings of the Royal Society of London A: Mathematical, Physical and Engineering Sciences **276**, 238 (1963).
- [37] M. C. Gutzwiller, Phys. Rev. Lett. **10**, 159 (1963).
- [38] R. Micnas, J. Ranninger, and S. Robaszkiewicz, Rev. Mod. Phys. **62**, 113 (1990).
- [39] J. E. Hirsch, Phys. Rev. B **28**, 4059 (1983).
- [40] E. Vitali, P. Rosenberg, and S. Zhang, Phys. Rev. A **100**, 023621 (2019).
- [41] S. Rossotti, M. Teruzzi, D. Pini, D. E. Galli, and G. Bertaina, Phys. Rev. Lett. **119**, 215301 (2017).
- [42] J. P. F. LeBlanc, S. Li, X. Chen, R. Levy, A. E. Antipov, A. J. Millis, and E. Gull, Phys. Rev. B **100**, 075123 (2019).
- [43] W. Zimmermann, R. Frésard, and P. Wölffe, Phys. Rev. B **56**, 10097 (1997).